Modeling and Analysis of Brushless Generator Based Biomechanical Energy Harvesting System

Ze'ev Rubinshtein
Department of Electrical and Computer Engineering
Ben-Gurion University of the Negev
Beer-Sheva, Israel
zeevrub@ee.bgu.ac.il

Raziel Riemer
Department of Industrial Engineering and Management
Ben-Gurion University of the Negev
Beer-Sheva, Israel
rriemer@bgu.ac.il

Shmuel (Sam) Ben-Yaakov
Department of Electrical and Computer Engineering
Ben-Gurion University of the Negev
Beer-Sheva, Israel
sby@ee.bgu.ac.il

***Abstract*— An analysis and modeling approach of an electro-mechanical harvesting system based on a brushless generator (BLG) is presented and evaluated. The approach is based on an electrical analog of the mechanical components and was verified by modeling a knee joint harvesting system. Good agreement was found between the model predictions and the experimental results. New harvesting strategies based on energy storage by the BLG moment of inertia are suggested and examined.**

NOMENCLATURE

B	core losses coefficient
C_r	rotors moment of inertia emulating capacitance
C_j	dummy capacitance load
C_g	gear moment of inertia emulating capacitance
E_i	i phase BEMF
F_L	output frequency
i	phase index
I_{em}	generator-induced torque emulating current
I_{in}	shaft external mechanical torque emulating current
I_{net}	shaft net torque emulating current
I_g	injected torque emulating current
I_i	i winding current
I_{gf}	gear friction emulating current
I_f	generator shaft friction emulating current
I_d	generator core losses emulating current
J	moment of inertia
K_e	BEMF constant
$K_{e_{rms}}$	BEMF constant for RMS voltage
K_t	moment constant
N	number of stator phases
L_i	i phase inductance
p	number of pair poles
R	dummy resistance load
R_L	load resistance
R_i	i phase resistance
T_{net}	shaft net torque
T_{in}	shaft external mechanical torque
T_{em}	generator-induced torque
T_f	friction
T_d	torque emulating core losses
T_i	i phase electro-magnetic torque
V_{θ^*}	unbound shaft mechanical angle emulating voltage
V_θ	shaft electrical angle emulating voltage
V_{in}	shaft angular frequency emulating voltage
V_T	input torque to gear low speed side
V_j	shaft angular velocity on gear's low speed side
V_L	load phase voltage
V_{Lrms}	RMS load phase voltage
θ	shaft mechanical angle
ω	shaft angular frequency

This research was supported by the ISRAEL SCIENCE FOUNDATION (Grants No. 476/08 and No. 517/11).

I. INTRODUCTION

With the increasing use of portable electronics, there is a growing demand for portable sources of power. One interesting emerging technology is biomechanical energy harvesting [1], [2]. This technology uses human natural motion, such as walking, to generate energy. The logic behind this approach is the fact that the energy density of food is 35-100 times higher than that of batteries (depending on the type of battery and food). Moreover, during one day of activity a person uses approximately 10.7MJ of energy, which, if stored electrically, would require 20Kg of batteries [3]. It is thus believed that harvesting small amounts of energy from human movement will not cause an appreciable additional metabolic load. This premise led to the development of various devices for generating energy from humans, such as heel strike devices that use energy from the compression of the shoe soul. Yet these devices can harvest at most 1W [3]. Rome and colleagues developed a spring-loaded backpack, weighing 38Kg that harnesses vertical oscillations to harvest 7.4W at a walking speed of 6.5km/h [4]. Another direction was proposed by Niu and colleagues [2]. Their idea utilizes the fact that muscles work in two different modes; positive work, where the muscles generate motions and negative work, where the muscles act as brakes to slow down the motion. Based on this concept, Niu and colleagues [2] proposed a knee joint device that is composed of a gear train and generator, which is active during negative

work and performs part of the braking torque instead of the muscles in a way that is similar to regenerative braking in an electric car. This device was later developed and built by Donelan et al. [1], [5]. The goal of such a device would be to generate as much energy as possible with minimal or no interference to the natural walking movements. Based on this objective, Li, et al. [5] proposed a method for designing a knee joint harvester that is based on a given motor, where the parameters for design optimization were gear ratio and external resistance [5]. Riemer et al. [6] presented a harvester device optimization method that also enables comparison between different motors. Hitherto, design and optimization methods consider only the static performance of the systems and lack the ability to exhibit the dynamic behavior of the devices. In a knee harvester, which is the device that was investigated in this study, dynamic behavior is of prime importance, considering the fact that the knee joint angular velocity and direction change during the gait cycle. Further, it is important that the braking torque applied to the knee will be smaller than the knee joint muscle torque during natural walking. If the braking torque is larger than the muscle torque the user will have to perform extra (positive) work to overcome this resistance. A dynamic model can also help optimize advanced modes of operation such as harvesting during angles of knee swing, in which negative work is performed by the muscles in a way that is similar to regenerative braking in an electric car [2].

The objective of this paper is to present a modeling approach for an electro-mechanical harvesting system that is based on a brushless generator (BLG). An important feature of the proposed modeling approach is its seamless compatibility with common circuit simulation software packages, such as SPICE-based simulators. This capability allows full examination of the system's dynamic behavior and can thus serve as a pivotal tool in the development of power management systems for the extraction of maximal power from a device. The proposed modeling methodology is demonstrated by considering a knee joint harvesting system (Fig. 1) that comprises an orthopedic knee brace, configured so that knee motion drives a gear train through a unidirectional clutch, transmitting only knee flexion motion to a BLG [6].

Figure 1. Knee energy harvesting - experimental prototype.

II. MODELING APPROACH

The modeling approach adopted in this study is based on electrical emulation of the mechanical part of the system. The simulator adopted in this study is Orcad v16.2, but any other simulator that includes dependent sources would be suitable. The relationships between the mechanical and electrical analogs are given in Table I.

The 3-phase BLG modeling is based on equations (1-5) listed below [7]. The mechanical rotation system equation (1) describes the relationship of the system's shaft net torque (T_{net}) and the system's acceleration/deceleration ($d\omega/dt$) according to the system's moment of inertia (J).The electric circuit analogue is shown in Fig. 2.

$$T_{net} = J\, d\omega/dt \rightarrow I_{net} = C\, dV_{in}/dt \quad (1)$$

The electrical analogue of the BLG shaft torque (2) consists of current sources connected in parallel with a single capacitor (C_r) that represents the rotors' moment of inertia (Fig. 3a). The dependent current sources represent the different torques: the shaft external mechanical torque (T_{in}), the generator-induced torque (T_{em}), which is a function of the phase current and shaft position, friction (T_f), which is assumed to be constant, and core losses (T_d) which are speed dependent. The expressions for these torques are given in eq. (3-4), while eq. (5) is the expression of the Back Electro Motive Force (BEMF), for which the amplitude and frequency are shaft-speed dependent.

$$T_{net} = T_{in} - T_{em} - T_d - T_f$$
$$\rightarrow I_{net} = I_{in} - I_{em} - I_d - I_f \quad (2)$$
$$T_d = B\omega \rightarrow I_d = BV_{in} \quad (3)$$
$$T_{em} = \sum_{i=1}^{N} T_i = \sum_{i=1}^{N} K_t\, I_i \sin(p\theta - (i-1)2\pi/N)$$
$$\rightarrow I_{em} = K_t \sum_{i=1}^{N} I_i \sin(V_\theta - (i-1)2\pi/N) \quad (4)$$
$$E_i = K_e\, \omega \sin(p\theta - (i-1)2\pi/N$$
$$\rightarrow E_i = K_e\, V_{in} \sin(V_\theta - (i-1)2\pi/N) \quad (5)$$

TABLE I. ANALOGY BETWEEN MECHANICAL AND ELECTRICAL QUANTITIES

Mechanical		Electrical	
variable	***unit***	***variable***	***unit***
ω	rad/sec	V	V
T	Nm	I	A
J	Kgm^2	C	F

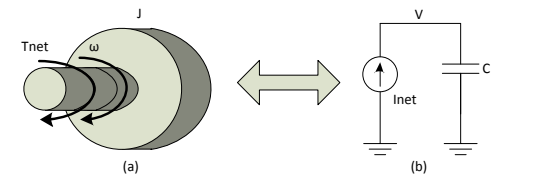

Figure 2. Mechanical to electronic analogy (a) mechanical system, (b) its electrical analog model.

where ω is the shaft angular frequency; V_{in} is the voltage representation of the shaft angular frequency; B is the core losses constant; i is the phase index; N is the number of stator phases; T_i is the i phase electro-magnetic torque; K_t is the moment constant; I_i is the i winding current; θ is the shaft mechanical angle; p is the number of pair poles; V_θ is the voltage representation of the shaft electrical angle; I_{em} is the current representation of the generator-induced torque; I_{in} is the current representation of the shaft external mechanical torque; I_d is the current representation of the generator core losses; I_f is the current representation of the friction; E_i is the i phase BEMF; K_e is the BEMF constant.

In the three-phase BLG machine considered in this study the stator windings are "Y" connected (Fig. 3b). Each phase can be represented by a sinusoidal BEMF voltage source (E_i) (5), inductance (L_i) and resistance (R_i). The circuits

presented in Fig. 3-5 are simplified schematics and not the actual simulation circuits. In the Orcad simulation schematics, the dependent voltage sources will be implemented by behaviorally dependent voltage source elements (EVALUE) and dependent current sources will be implemented using behaviorally dependent current source elements (GVALUE).

The dependent sources E_i, I_{em} (4-5) are functions of the shaft angle, which is unavailable in the electrical model of the BL machine (Fig. 3a, 3b). The angle was obtained by integrating the bus voltage that represents the angular frequency. This is accomplished by an auxiliary circuit (Fig. 3c) which produces the signal (V_{θ^*}) that emulates the unbound shaft mechanical angle. To obtain the electrical angle (V_θ) in the range of [0,2π], a modulo function (6) has been implemented by another auxiliary circuit with a behavioral voltage source (Fig. 3d). In these auxiliary circuits (Fig. 3c, 3d), voltage represents angle in radians. The resistance (R) in auxiliary circuits (Fig. 3d, 3e) is a dummy resistance needed for the simulation.

$$V_\theta = pV_{\theta^*} - 2\pi \left\lfloor \frac{pV_{\theta^*}}{2\pi} \right\rfloor \quad (6)$$

The electrical signal (V_θ) that represents the shaft's electrical angle is used by yet another auxiliary circuit (Fig. 3e) to generate the logic signals of the three built-in Hall Effect sensors of the BLG that are 120º apart and used for synchronizing the phase commutations. The logic functions of the Hall Effect sensors were implemented by EVALUE using IF statements.

The full electro-mechanical model is depicted schematically in Fig. 4. The model includes a front end section (Part A) that translates the knee joint angle to shaft torque, which is the required input to the motor (Fig. 3a). This is accomplished by two cascaded feedback loops. The first one (Fig.4a) includes translation of the angle ($V_{\theta ref}$) to angular velocity ($V_{\omega ref}$), as direct differentiation will introduce noise it is avoided by using a closed loop with integration in the feedback. The transfer function of the first loop is of first order, the loop's plant is a constant (K_1) equal to 500 for a fast and strong response. The second loop produces the input torque (V_T) to the motor, while minimizing the error between the required rotational speed, as calculated by first section, and the actual shaft angular velocity (V_j) on the low speed side of the gear train. As in the first loop, the transfer function is of first order if the friction losses of the gear train and the BLG are neglected. The constant K_2 is introduced to amplify the loop's response and its value is 100. Because of the unidirectional gear, Part A can only accelerate the BLG and the loop's response should be fast and strong enough to withstand any required acceleration. However, it must not overshoot as correction is not possible. Part B of the electro-mechanical model (Fig. 4b) includes the injected torque from part A (I_g) on the high

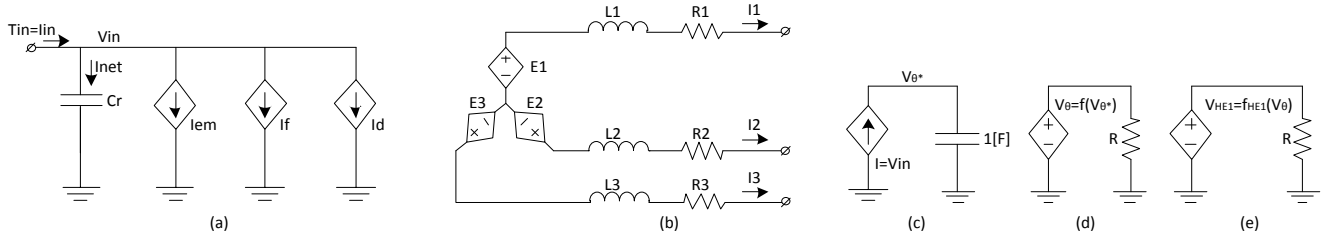

Figure 3. BLG modeling circuitry (a) electrical analog of mechanical shaft, (b) 3 phase stator, (c) shaft position detector, (d) shaft position to electrical angle converter, (e) Hall Effect sensor emulator.

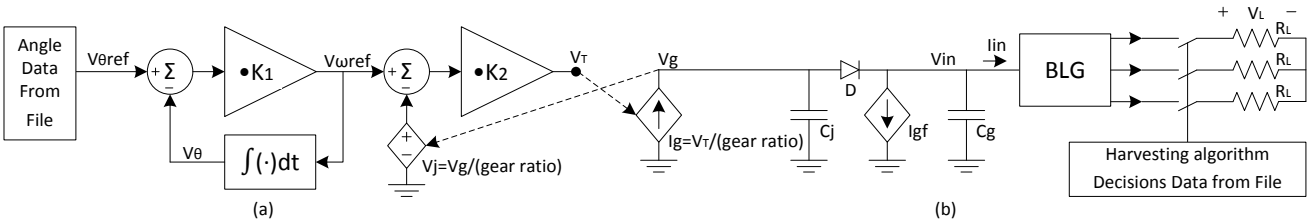

Figure 4. Model of the complete electro-mechanical system and its simulation control block, (a) simulation control block, (b) electro-mechanical system.

speed side of the gear train and a dummy load (C_j) needed for simulation. The gear train friction (I_{gf}) value was found by simulation calibration to be 1mA and the moment of inertia (C_g) has been given by the manufacturer as 430nF on the high speed side. The "Y" connected balanced load resistors (R_L) are connected via three switches that are activated according to the harvesting scheme. The torque excitation is connected to the BLG block via an ideal diode to emulate the behavior of the unidirectional gear. The angle data and harvesting decision data are stored in tab delimited files and are imported to the simulation using voltage piecewise linear sources (VPWL_FILE).

III. Experimental Results

The basic data of the experimental BL machine (EC-45 flat, Table II, [8]), when operated as a generator, was verified experimentally by driving it by another motor and loading the BLG with three, star connected rheostats (R_L) set to values of 0.92, 2, 5, 10 and 20 Ω. Each load was tested for a series of rotational speeds up to 4000rpm and the load voltages and frequencies were recorded. The experimental results showed a frequency-independent linear behavior which suggests that the winding inductance can be neglected in a system that operates in the expected (and tested) angular speed region. The measured phase load voltage (V_{Lrms}) and frequency (F_L) were used to extract the BEMF constant (K_{erms} V/rpm) and winding resistance (R_i) by the following procedure. The load voltage per phase was expressed as a function of the BEMF constant, phase frequency, number of pole pairs (p), winding resistance and load resistance (R_L):

$$V_{Lrms} = K_{e_{rms}}\left(\frac{F_L}{p} * 60\right)\left(\frac{R_L}{R_L+R_i}\right) = K_{e_{rms}} n \left(\frac{R_L}{R_L+R_i}\right) \quad (7)$$

where n is the rotor rotational speed in rpm.

Next, (7) was rearranged as a linear equation $y = ax + b$ where '$x = (nR_L/V_{Lrms})$' and '$y = R_L$' are known values:

$$R_L = K_{erms}\,(nR_L/V_{Lrms}\,) - R_i \quad (8)$$

The linear trend line of all the experimental results (Fig. 6) was used to estimate the BEMF constant (K_{erms}) and the winding resistance (R_i). They were found to be $K_{erms} = 0.0011\ \mathrm{V_{rms}/rpm}$ and R_i= 0.357 Ohm. The BEMF constant is in good agreement with the manufacturer's specifications when a factor of $\sqrt{6}$ is taken into account since we consider the BEMF of each phase for RMS voltage while the manufacturer cites the speed constant for the peak voltage between phases. The phase resistance that was found here includes the wires' and connectors' resistances of the experimental system and has no effect on the BEMF constant. The phase-to-phase resistance and inductance were measured using an INSTEK RLC meter and found to be 0.445 Ohm and 0.28mH.

Simulations were run to test the validity of the model parameters. In these simulations the motor rotational speed was controlled by a feedback loop that measures the actual speed, compares it to the desired value (profile of angular velocity at knee during walking) and generates the input

TABLE II. Relevant parameters of BL motor*

Nominal voltage	18 V
No load speed	6710 rpm
No load current	294 mA
Nominal speed	5250 rpm
Nominal torque	96.9 mNm
Nominal current	3.54 A
Terminal resistance phase to phase	0.413 Ohm
Terminal inductance phase to phase	0.322 mH
Torque constant	25.1 mNm/A
Speed constant	380 rpm/V
Rotor inertia	135 gcm2

*extracted from manufacturer datasheet [8]

torque to the machine via a PID compensator (Fig. 5). PID values ($K_P = 1000, K_I = 1000, K_D = 0.1$) were chosen so that the system will be stable, but they are not optimized for dynamic response as the requested parameters (BEMF constant and phase resistance) are extracted in steady state and the transient response is ignored. The simulation results are included in Fig. 6 and show less than 5% deviations from the experimental results.

The experimental data of the knee harvester was obtained from 8 volunteers, each equipped with two knee harvesters, who walked on a treadmill at different speeds (4,5,6 km/h).

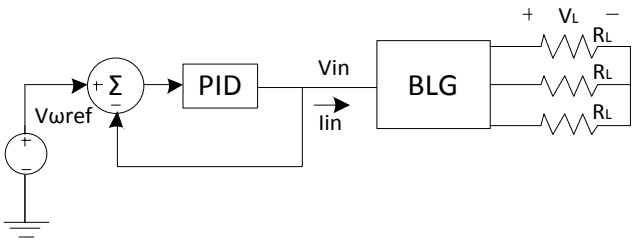

Figure 5. Simulation circuit for BLG model parameters extraction.

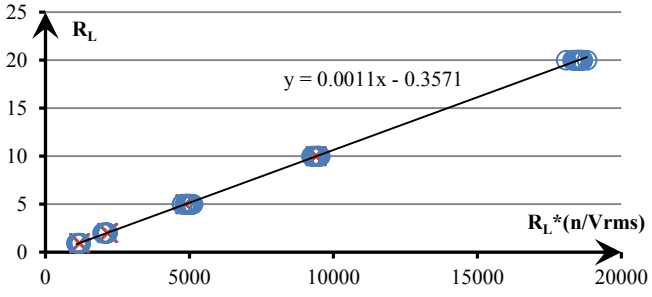

Figure 6. BLG experimental and simulation results. Cross markers – simulation results, circle markers – experimental measurements, solid line – linear fit based on experimental measurements, equation– fitting result.

The data from both knee devices were sampled by a Tektronix SCOPE 2014B whose data logged using NI LabVIEW Signal Express 3 software. The joint angle data was fitted to a 11th order polynomial curve to reduce noise and to facilitate a continuous input to the simulation model by MATLAB script. The mechanical losses of the gear (I_{gf}) and BLG (friction and core) were estimated by fitting the simulation results to the measured load phase voltage for different subjects at different walking paces. Once calibrated, the model was found to accurately replicate all the experimental results, as shown in Fig. 7 for one case. Comparison of the total energies showed a difference of less than 10%. All important simulation parameters are summarized in Table III.

The ability of the model to serve as a tool for analyzing and optimizing electro-mechanical harvesters is demonstrated in Fig. 8. Fig. 8a shows how the simulated knee angle of the model follows the given angle profile (the traces are on top of each other). Fig. 8b presents the measured and simulated generator rotational speed on the knee side of the gear train. The plots show perfect match until the point where the knee angle angular velocity starts to decline rapidly (Fig 8a, at around 270ms). At this point, the clutch disengaged and the generator continued to spin by inertia. In this particular experiment the generator's rotational speed was accelerated and when it reached maximum speed (at around 150ms) the generator was loaded by a three 2Ω resistors. The mechanical torque imposed on the knee in this mode of operation includes two sections: i) during motor acceleration as the angular velocity was building up (Fig. 8c, the section from 50ms to 150ms) and ii)

TABLE III. SIMULATION PARAMETERS

Gear Ratio	83
Gear moment of inertia	4.3 gcm^2
Gear friction on the high speed side	1 mNm
Phase resistance	0.22 Ohm
Phase inductance	0.12 mH
BEMF constant	0.0011 Vrms/rpm
Torque constant	14.855 mNm/A
Core losses constant	0.01 mNm/(rad/sec)
Rotor friction	1 mNm
Wire resistance	0.3 Ohm

during the harvesting period (the section from 150ms to about 230ms). The maximum torque (on the generator's side) in this mode of operation was about 60mNm while the torque during harvesting was about 30mNm, which translates to the knee side as 5.7Nm and 2.85Nm respectively. Considering the fact that knee torques are around 15Nm [3], the perturbation of the harvesting device torque is only about 1/5 of the prevailing torque. The phase voltage during harvesting shown in Fig. 8d was used to calculate the total output energy per phase for one stroke (Fig. 8e). These data imply that in this mode of operation about 1.2J could be harvested per stride (three phases of two knee devices). This conclusion was verified by an experiment conducted on the device and shown in Fig. 1.

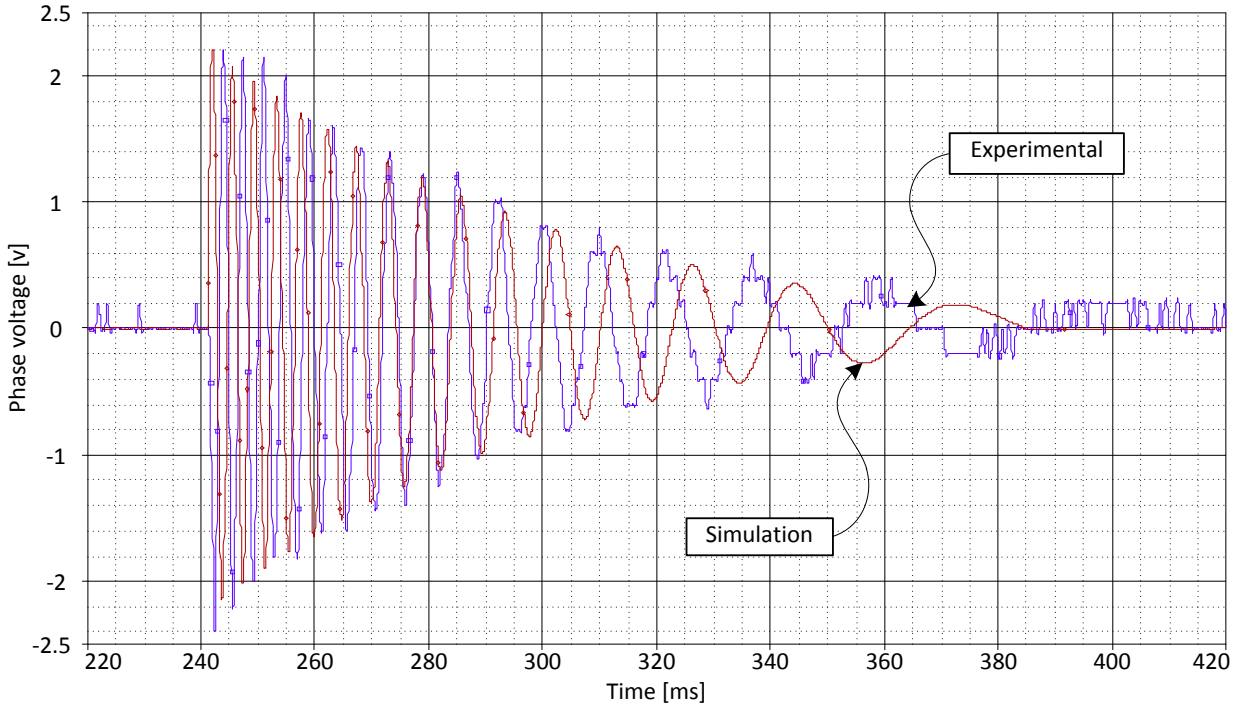

Figure 7. Simulation and experimental results for load voltage of a single phase during the harvesting

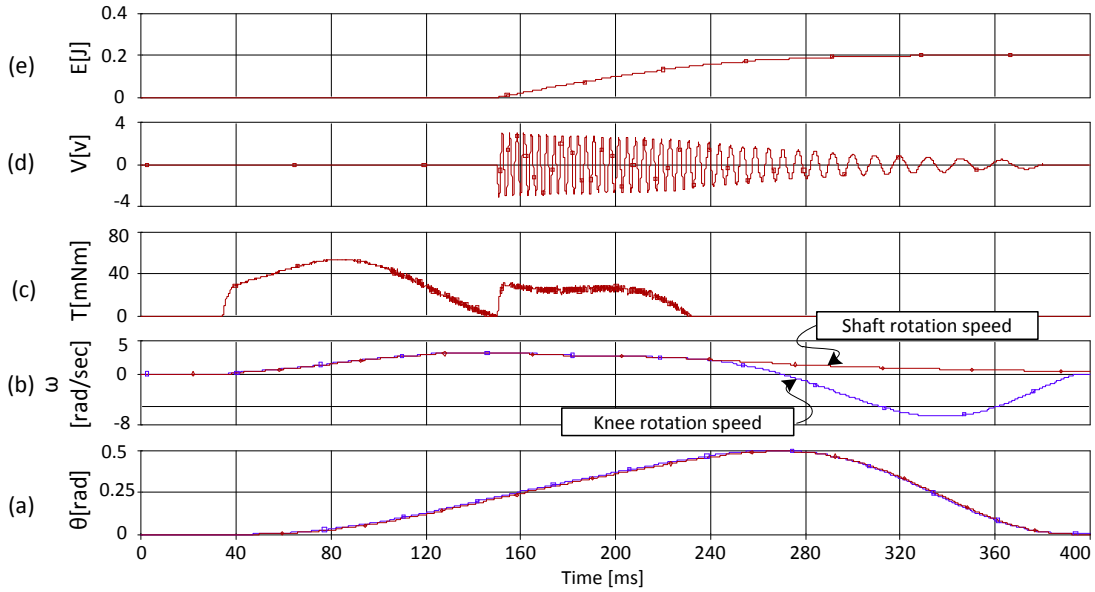

Figure 8. Example of simulation model prediction capabilities, (a) the input knee angle profile and the tracked emulated angle generated by the model (the traces are on top of each other), (b) knee and motor normalized rotation speed, (c) torque applied to the shaft, (d) load voltage of a single phase, (e) accumulated energy from a single phase.

IV. Discussion And Conclusions

This work introduces a modeling approach for electro-mechanical systems using an electrical simulator such as SPICE-based software. Simulations based on the model revealed that the moment of inertia of the BLG plays an important role in the behavior of the harvesting system and that it can be used for temporary energy storage to be expended at a later time. For example, by delaying the energy-harvesting until after the acceleration phase (Fig. 8), the momentary torque imposed on the knee can be made smaller, as compared to the case where acceleration and harvesting are concurrent. This strategy is appropriate in the case of a BLG with a relatively large moment of inertia, such as the machine used in this study. While this approach allows for higher energy production it limited to fix gait cycles. When using the device at variable gait patterns, like walking on flat surface and then climbing stairs, generators with smaller moments of inertia that fit the requirements of small size and weight and of high efficiency would be probably better. Yet, for both cases the proposed model could be used to optimize the modes' operation.

Aside from applying the model for studying the electro mechanical interaction of the harvesting device, the model can be used to optimize the power management that needs to be performed between the BLG and practical loads – such as a chargeable battery. Although only demonstrated on a knee joint harvesting device, the proposed approach can be used to model other electro-mechanical harvesting systems, such as heel strike or center of mass movement [3].

References

[1] J. M. Donelan, Q. Li, V. Naing, J. A. Hoffer, D. J. Weber, and A. D. Kuo, "Biomechanical energy harvesting: generating electricity during walking with minimal user effort," Science, vol. 319, no. 5864, pp. 807-810, 2008.

[2] P. Niu, P. Chapman, R. Riemer, and X. Zhang, "Evaluation of motions and actuation methods for biomechanical energy harvesting," IEEE 35th Annual Power Electronics Specialists Conference, 2004. PESC 2004. vol. 3, pp.2100-2106, 2004.

[3] R. Riemer and A. Shapiro, "Biomechanical energy harvesting from human motion: theory, state of the art, design guidelines, and future directions," J. of Neuroengineering and Rehabilitation, vol. 8, no. 22, doi:10.1186/1743-0003-8-22, Apr. 2011.

[4] L. C. Rome, L. Flynn, E. M. Goldman, and T. D. Yoo, "Generating electricity while walking with loads," Science, vol. 309, no. 5741, pp. 1725-1728, 2005.

[5] Q. Li, V. Naing, and J. M. Donelan, "Development of a biomechanical energy harvester," J. of Neuroengineering and Rehabilitation, vol. 6, no. 22, doi:10.1186/1743-0003-6-22, Jun. 2009.

[6] R. Riemer, A. Shapiro, and S. Azar, "Optimal gear and generator selection for a knee biomechanical energy harvester", 1st International Conference on Applied Bionics and Biomechanics, Venice, Italy, 2010.

[7] J. F. Gieras and M. Wing, Permanent Magnet Motor Technology, 2nd ed., New York: Marcel Dekker, 2002.

[8] Maxon EC 45 flat 339285 Datasheet, Maxon Motor Co., Switzerland, 2012. http://www.maxonmotor.com/medias/sys_master/8796893708318/EC-45-flat-339285_11_EN_194.pdf